ELSEVIER

Materials Characterization 58 (2007) 401 – 405

MATERIALS CHARACTERIZATION

Short communication

Large-scale fabrication of ZnO nanocrystals by a simple two-step evaporation–oxidation approach

Shou-Chian Hsu, Wha-Tzong Whang *, Chin-Hsien Hung

Institute of Materials Science and Engineering, National Chiao Tung University, 1001 Ta Hsueh Road, Hsin Chu, Taiwan 300, Republic of China

Received 4 May 2006; accepted 5 June 2006

Abstract

Single crystal structures of ZnO nanocrystals were prepared on quartz and polyimide (PI) film substrates by using a thermal coater to promote thermal evaporation, followed by air circulation at 350 °C for 2 h to effect oxidation. HRTEM and TEM images show the individual ZnO nanocrystals have regular lattice order without stacking faults. After dispersion by an ultrasonic bath, ZnO deposited on PI film substrates can consist of individual and well-distributed nanocrystals with an average crystal size of 20–30 nm. In photoluminescence, the nanocrystalline ZnO exhibits strong UV emission at 395 nm, with no emission in the visible spectrum. The synthetic method described in this paper provides a simple and efficient method to fabricate ZnO nanocrystals on a large scale.

Keywords: Crystal morphology; Physical vapor deposition processes; Zinc compounds

1. Introduction

Semiconductor nanocrystals have wide application for electronic and optoelectronic devices because of their unique quantum confinement effects. In recent years, zinc oxide (ZnO) has attracted much attention due to its excellent physical properties, such as a wide band gap (3.37 eV) at room temperature and large exciton bonding energy (60 meV). It can be applied to ultraviolet light-emitting diodes, transparent electrodes and piezoelectric devices, etc. Many different methods have been reported for the fabrication of ZnO nanocrystals: sol–gel techniques [1], chemical vapor deposition (CVD) [2], thermal decomposition [3], spray pyrolysis [4] and RF plasma deposition [5]. Thermal evaporation is one of the simpler ways to prepare ZnO nanostructures. Many researchers have reported using horizontal high-temperature tube furnaces to fabricate different morphological ZnO nanostructures [6–11]. Yu et al. [6] have prepared ultraviolet-emitting ZnO nanowires by thermal evaporation of zinc powder mixed with selenium powder. Wang et al. [7] successfully synthesized ZnO nanowires, nanoribbons, and needle-like rods via thermal evaporation of a mixture of ZnO powder and graphite. A nanoribbon junction of ZnO has been fabricated by using a mixture of ZnO and SnO_2 powders as the source materials. Roy's group [8] has reported the morphology and luminescent properties of ZnO nanostructures prepared by thermal evaporation of Zn under various conditions.

However, most of the preparation of ZnO nanostructures by thermal evaporation is restricted to fabricating small amounts in a high temperature horizontal furnace. In

* Corresponding author. Tel.: +886 3 5731873; fax: +886 3 5724727.
E-mail address: wtwhang@mail.nctu.edu.tw (W.-T. Whang).

1044-5803/$ - see front matter © 2006 Elsevier Inc. All rights reserved.
doi:10.1016/j.matchar.2006.06.001

this paper, we report using a convenient thermal coater to effect thermal evaporation, followed by air circulation to cause oxidation to successfully fabricate ZnO nanocrystals at low temperature on quartz and flexible polyimide (PI) film substrates. The structure and photoluminescence properties have been studied in this paper.

2. Experimental procedure

Appropriate amounts of pure ZnO powder (99.99% purity) was placed in a tungsten boat and thermally evaporated on the quartz or PI substrates in a vacuum chamber at 5×10^{-6} Torr. The deposition rate was controlled by the boat temperature and stabilized at 1 Å/s. We further oxidized the as-deposited ZnO products at 350 °C for 2 h under air-circulation. The fabricated products were analyzed by a X-ray powder diffraction (XRD) with CuKα radiation (MacScience, MXP), a field-emission scanning electron microscope (FE-SEM) (Hitachi, JSM-6500F), a transmission electron microscope (TEM) (Philips, Jecnai 20), and a high resolution TEM (HRTEM) (Philips, Jecnai 20). The specimens for TEM and HRTEM were prepared by dispersing the products in methanol using an ultrasonic bath, and depositing the suspension onto carbon film-coated copper grids. The photoluminescence (PL) characteristic was measured by Hitachi F4500 spectrofluorophotometer with the excitation wavelength at 325 nm.

3. Results and discussion

Fig. 1 shows the XRD patterns of the sample, as-deposited and after oxidization. The as-deposited product displays the main diffraction peaks for metallic zinc at $2\theta=36.3°$, 39.1° and 43.3°, which correspond to the (002), (100) and (101) planes of hexagonal Zn; no diffraction peaks of ZnO are observed. We believe that Zn–O bonding of the source materials is damaged by the thermal evaporation process. On the basis of stoichiometry, the probability for zinc and oxygen atoms to react to form ZnO would be relatively low in a large vacuum chamber. Moreover, oxygen atoms have a lower atomic weight than zinc atoms and could be easily removed by the vacuum treatment. Also in Fig. 1, after oxidation at 350 °C for 2 h, diffraction peaks of metallic zinc were not detected. Instead, the main diffraction peaks corresponding to (100), (002) and (101) planes of ZnO with a hexagonal wurtzite structure were detected. This means that metallic zinc products are rapidly transformed into ZnO crystals at low temperature by using air circulation.

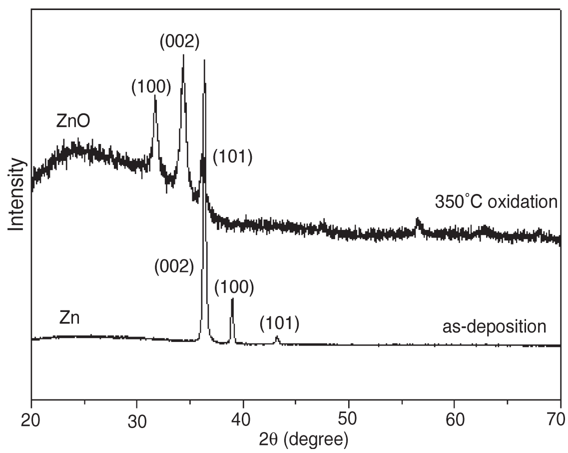

Fig. 1. XRD pattern of ZnO samples as-deposited and after oxidation at 350 °C for 2 h.

Fig. 2 shows top view and side view FE-SEM images of the samples deposited on quartz substrates for deposition times of 2 min, 5 min and 10 min, respectively, and then oxidized at 350 °C for 2 h. From Fig. 2 (a)–(c), it can be seen that the ZnO products consist of nanocrystals, and crystal aggregation becomes more prominent with increasing deposition time. The average sizes of the crystal aggregates increase from 20–40 nm at the 2 min deposition, to 60–80 nm at 5 min, and 120–150 nm at 10 min. In addition, we can observe clearly the morphology transformation of the fabricated ZnO nanostructures by the side view FE-SEM images presented in Fig. 2(d)–(f). When the deposition time is increased from 2 min to 5 min, the morphology of ZnO nanostructures transform from an “island shape” to densely aggregated nanoparticles. Rod-like nanostructures were observed after the 10 min deposition.

Some literature has commented upon the mechanism of crystal growth. Matijevic et al. [12] reported a two-stage growth, in which primary particles are formed first via nucleation and growth, and continue to aggregate with time to develop secondary particles. Oliveira et al. [13] mentioned that particle aggregation would favor a *c*-axis orientation, probably because of crystal polarity. In the present case, we suggest that the morphology of ZnO nanostructures are formed before the oxidization process although the main composition of as-deposited products is metallic zinc. Metallic zinc and ZnO have the same hexagonal structure. After oxidization, oxygen atoms occupy one-half of the tetrahedral sites in the hexagonal zinc structure, and then develop into ZnO with the wurtzite hexagonal structure. Hence, only the lattice volume is increased after oxidization because of oxygen incorporation [14].

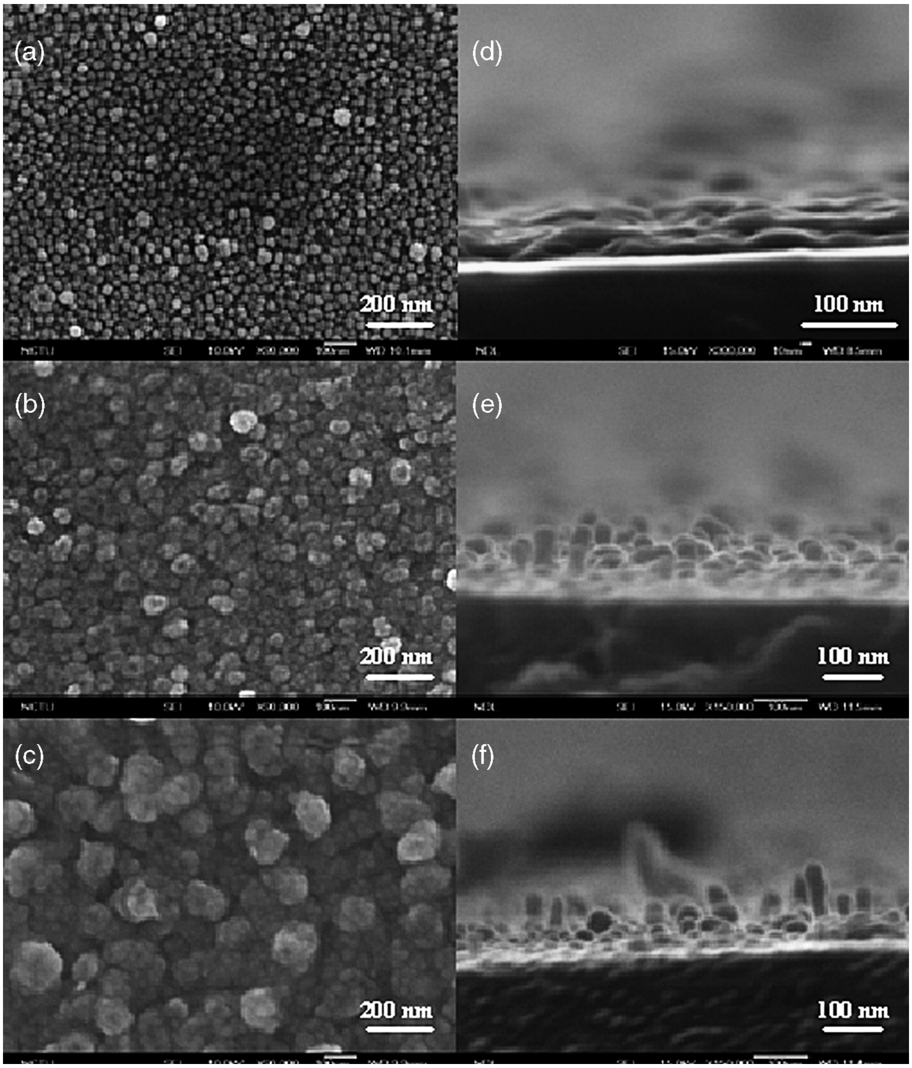

Fig. 2. Top view (a–c) and side view (d–e) FE-SEM images of ZnO samples fabricated on quartz substrates at three different deposition times: 2 min, 5 min and 10 min, respectively, and then oxidized at 350 °C for 2 h.

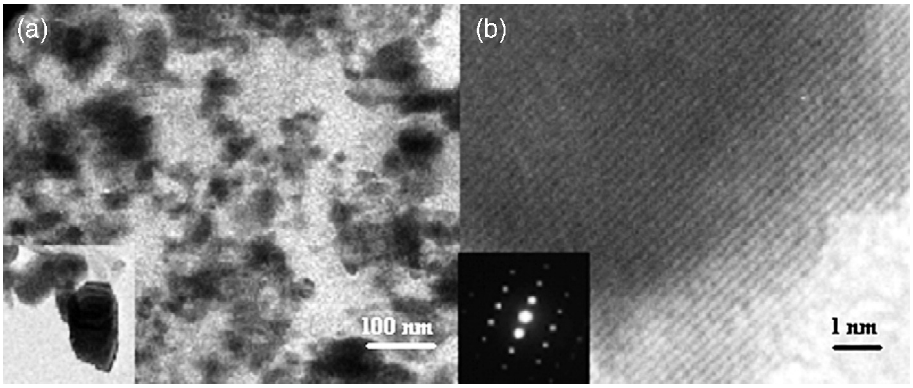

Fig. 3. (a) Low magnification TEM image of the ZnO nanocrystals and high magnification TEM images (inset); (b) HRTEM image and the SAED pattern (inset).

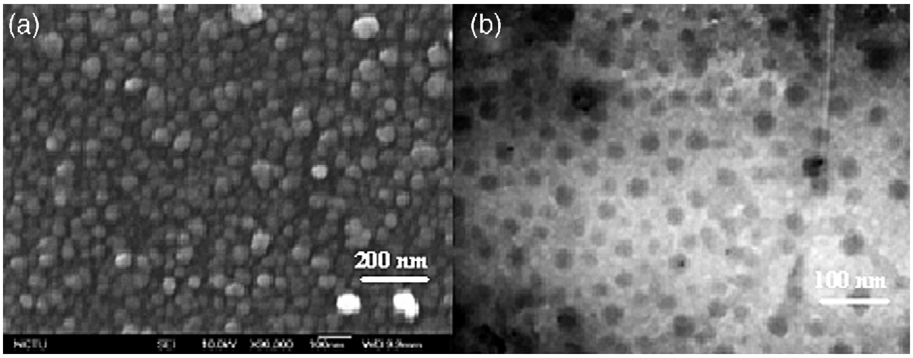

Fig. 4. (a) FE-SEM images of the ZnO samples fabricated on PI substrates; (b) TEM image of the same sample.

The detailed microstructural features of ZnO nanocrystals which were deposited for 10 min on quartz substrates were further studied by TEM. As shown in Fig. 3(a), the sample shows partial aggregation and the aggregate distribution is not uniform, but the average sizes of the crystal aggregates were smaller than those observed by FE-SEM, and no rod-like structures were found. This suggests that the ultrasonic bath scatters the agglomerated ZnO nanocrystals to cause loose structures. From the high magnified image (inset in Fig. 3(a)) and the selected area electron diffraction pattern (inset in Fig. 3(b)), the individual ZnO nanocrystal presents a regular hexagonal shape and clear lattice fringes, indicating that it is a single crystalline structure. The HRTEM images are shown in Fig. 3(b). It can be seen that the ZnO nanocrystal exhibits regular lattice order without stacking faults, and the spacing between adjacent lattice planes is about 2.6 Å, which corresponds to the (002) plane.

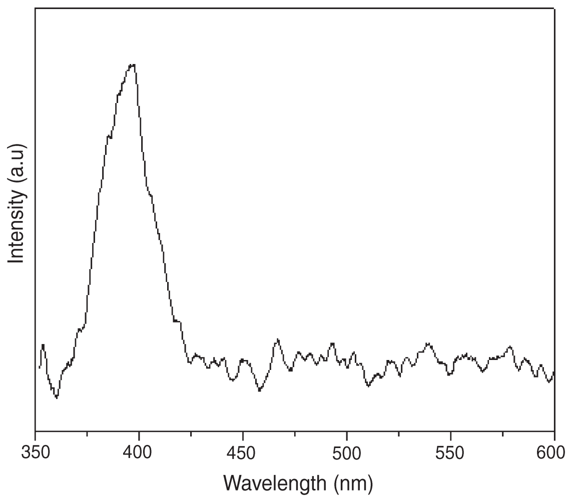

Fig. 5. Room temperature PL spectra of the ZnO nanocrystals deposited for 10 min on quartz substrates.

Because the process occurs at relatively low temperature, we further prepared ZnO nanocrystals on PI film substrates. Fig. 4 shows the FE-SEM and TEM images of ZnO nanocrystals which were deposited for 10 min. From Fig. 4(a), it is seen that the sizes of the crystal aggregates are smaller than those on quartz substrates, Fig. 2(c). Also, after ultrasonic dispersion for 10 min, the TEM image, Fig. 4(b), shows individual and well distributed 20–30 nm nanocrystals. This may suggest that ZnO deposits "harder" on organic PI film substrates than on quartz substrates and results in lower adsorbability, and less significant crystal aggregation. Because PI films are flexible and thermally stable, this method offers the means for mass production of ZnO nanocrystals on roll-type PI films.

Published literature reports that two emission band characteristics of ZnO nanostructures arise from different processes: the ultraviolet (UV) band emission results from near band-edge emission, while the green band emission has been attributed to structural defects such as oxygen vacancies [15,16]. Fig. 5 shows the room temperature photoluminescence spectra of the ZnO nanocrystals deposited 10 min on a quartz substrate. The resulting ZnO nanocrystals exhibit strong UV emission at 395 nm; no emission in the visible spectrum, which might be attributable to oxygen defects, was detected. Conversely, the air-circulating oxidation environment results in nearly defect-free ZnO nanocrystals.

4. Conclusions

We have successfully prepared ZnO nanocrystals by using a thermal coating process followed by air circulation to effect oxidation. Air circulation provides a mild and rapid means for producing ZnO crystals, so flexible and thermally stable PI films, as an alternate to quartz substrates, can be used for the substrate. HRTEM and photoluminescence measurements show the resulting

ZnO nanocrystals are nearly defect-free single crystalline structures. In addition, the ZnO deposited on PI film substrates are present as individual and well distributed nanocrystals after dispersion by an ultrasonic bath. Because a roll-type of PI film can be used as a substrate for the continuous deposition of the ZnO, it can be a simple and efficient method for the large-scale fabrication of ZnO nanocrystals.

Acknowledgements

The authors gratefully acknowledge the National Science Council of the Republic of China NSC 92-2216-E-009-003 and the Lee and MTI center in NCTU for the financial support of this work.

References

[1] Chakrabarti S, Ganguli D, Chaudhuri S. Photoluminescence of ZnO nanocrystallites confined in sol–gel silica matrix. J Phys D Appl Phys 2003;36:146–51.

[2] Kim SW, Fujita S. Self-organized ZnO quantum dots on SiO_2/Si substrates by metalorganic chemical vapor deposition. Appl Phys Lett 2002;81:5036–8.

[3] Cozzoli PD, Curri ML, Agostiano A, Leo G, Lomascolo M. ZnO nanocrystals by a non-hydrolytic route: synthesis and characterization. J Phys Chem B 2003;107:4756–62.

[4] Panatarani C, Lenggoro IW, Okuyama K. Synthesis of single crystalline ZnO nanoparticles by salt-assisted spray pyrolysis. J Nanopart Res 2003;5:47–53.

[5] Sato T, Tanigaki T, Suzuki H, Saito Y, Kido O, Kimura Y, et al. Structure and optical spectrum of ZnO nanoparticles produced in RF plasma. J Cryst Growth 2003;255:313–6.

[6] Kong YC, Yu DP, Zhang B, Fang W, Feng SQ. Ultraviolet-emitting ZnO nanowires synthesized by a physical vapor deposition approach. Appl Phys Lett 2001;78:407–9.

[7] Yao BD, Chan YF, Wang N. Formation of ZnO nanostructures by a simple way of thermal evaporation. Appl Phys Lett 2002;81:757–9.

[8] Roy VAL, Djurisic AB, Chan WK, Gao J, Lui HF, Surya C. Luminescent and structural properties of ZnO nanorods prepared under different conditions. Appl Phys Lett 2003;83:141–3.

[9] Lee JS, Park K, Kang MI, Park IW, Kim SW, Cho WK, et al. Abnormal piezoresponse behavior of $Pb(Mg_{1/3}Nb_{2/3})O_3$–30% $PbTiO_3$ single crystal studied by high-vacuum scanning force microscope. J Cryst Growth 2003;254:423–6.

[10] Chen X, An C, Liu J, Wang W, Qian Y. Fabrication and characterization of hexagonal wire-like ZnO. J Cryst Growth 2003;253:357–60.

[11] Xie SS, Yuan HJ. Characterization of zinc oxide crystal nanowires grown by thermal evaporation of ZnS powders. Chem Phys Lett 2003;371:337–41.

[12] Park J, Privman V, Matijevic E. Model of formation of monodispersed colloids. J Phys Chem B 2001;105:11630–5.

[13] Oliveira APA, Hochepied JF, Grillon F, Berger MH. Controlled precipitation of zinc oxide particles at room temperature. Chem Mater 2003;15:3202–7.

[14] Kim TW, Kawazoe T, Yamazaki S, Lim J, Yatsui T, Ohtsu M. Room temperature ultraviolet emission from ZnO nanocrystallites fabricated by the low temperature oxidation of metallic Zn precursors. Solid State Commun 2003;127:21–4.

[15] Huang MH, Wu Y, Feick H, Tran N, Weber E, Yang P. Catalytic growth of zinc oxide nanowires by vapor transport. Adv Mater 2003;13:113–6.

[16] Geng BY, Xie T, Peng XS, Lin Y, Yuan XY, Meng GW, et al. Large-scale synthesis of ZnO nanowires using a low-temperature chemical route and their photoluminescence properties. Appl Phys A 2003;77:363–6.